MICROSTRUCTURAL STUDY OF THE TITANIUM ALLOY OXIDATION UNDER CREEP TEST

Danieli A. P. Reis
Instituto Tecnológico de Aeronáutica, ITA, São José dos Campos 12228-900, Brazil
danielireis@hotmail.com

Cosme R. M. da Silva
Universidade de Brasília, UNB, Brasília, 70910-900, Brazil.
Instituto Tecnológico de Aeronáutica, ITA, São José dos Campos 12228-900, Brazil
cosmeroberto@gmail.com

Miguel J. R. Barboza
Escola de Engenharia de Lorena, DEMAR 12600-000, Lorena, Brazil
mibarboza@uol.com.br

Francisco Piorino Neto
Comando-Geral de Tecnologia Aeroespacial, IAE, São José dos Campos 12228-904, Brazil
fpiorino@iae.cta.br

Carlos de Moura Neto
Instituto Tecnológico de Aeronáutica, ITA, São José dos Campos 12228-900, Brazil
mneto@mec.ita.br

Abstract. *Ti-6Al-4V is currently used in aeronautic and aerospace industry mainly for applications that require resistance at high temperature such as, blades for aircraft turbines and steam turbine blades. The titanium affinity by oxygen is one of main factors that limit the application of their alloys as structural materials at high temperatures. Notables advances have been observed in the development of titanium alloys with the objective of improving the specific high temperature strength and creep-resistance properties. However, the surface oxidation limits the use of these alloys in temperatures up to 600ºC. The objective of this work was evaluating the microstructure of the Ti-6Al-4V alloy in creep test. Yttria (8 wt.%) stabilized zirconia (YSZ) (Metco 204B-NS) with a CoNiCrAlY bond coat (AMDRY 995C) was atmospherically plasma sprayed on Ti-6Al-4V substrates by Sulzer Metco. Constant load creep tests were conducted with Ti-6Al-4V alloy in air and in nitrogen atmospheres in uncoated samples and in air in coated samples at stress level of 520 MPa at 500°C. The microstructural analyze show that the predominant mechanism in the test conditions was characterized by formation and coalescence of micro cavities with shape and size varieties. The cavities are corrugated in discontinue regions, like inclusions and points involving dislocation. The size and shape of dimples are governed by number and distribution of nucleated micro cavities and by stress internal level present in the material.*

Keywords: *Ti-6Al-4V, creep, oxidation, plasma-sprayed coatings*

1. Introduction

The search for alloys with improved high-temperature specific strength and creep-resistance properties for aerospace applications has led in the last decades to sustained research activities to develop new alloys and/or improve existing ones [1-3]. Titanium and its alloys are excellent for applications in structural components submitted to high temperatures owing to their high strength to weight ratio, good corrosion resistance and metallurgical stability. Its high creep resistance is great importance in enhancing engine performance [4,5]. However, the affinity by oxygen is one of main factors that limit its application as structural material at high temperatures. The high solid solubility of oxygen in titanium results in material loss and in the formation of hard and brittle layer during elevated temperature air exposure. [6,9]. The development of titanium alloys with the objective of improving the creep properties have been observed, although the surface oxidation limits the use of these alloys in temperatures up to 600°C [10,11]. A substantial part of the creep research has been devoted to Ti-6Al-4V alloy due to its industrial and technological importance. Its creep properties in air have been well documented. However, its creep behavior in nitrogen atmosphere has only rarely been investigated [12-15].

2. Experimental Procedure

The microstructural characterization of optical and electronic microscopy was a value instrument to comprehension of creep mechanism. The microstructural characterizations were done in samples coated and uncoated after creep test and consists in an evaluation of possible variations of microstructures and characteristics of the fracture surface. To the fractographic and microstructural analysis were used representative samples of creep test. Yttria (8 wt.%) stabilized zirconia (YSZ) (Metco 204B-NS) with a CoNiCrAlY bond coat (AMDRY 995C) was atmospherically plasma sprayed on Ti-6Al-4V substrates by Sulzer Metco. Constant load creep tests were conducted with Ti-6Al-4V alloy in air and in nitrogen atmospheres in uncoated samples and in air in coated samples at stress level of 520 MPa at 500°C.

The samples preparation to analysis by optical and electronic microscopy (MEV) followed the standard method of metallographic, like hot cupping (150ºC) under 21 MPa, after manual sanding with sandpaper of SiC, in sequence of 120, 240, 320 400, 600 and 1200 mesh. The polishing was done with colloidal silicon solution (OP-S). The MEV images were obtained in back-scattered electron mode. It was used a Leica optical microscope DMRXP model, ZEISS stereoscopy Stemi SV11 model, LEO scanning electronic microscopy 435 VPI model and JEOL scanning electronic microscopy JFM-5310 model.

3. Results and discussion

The Fig.1 shows a Ti-6Al-4V alloy micrographic as received. The microstructure consists of equiaxed α (HC) grains with average size about 10 μm. The β (CCC) phase is present in the α grain boundaries.

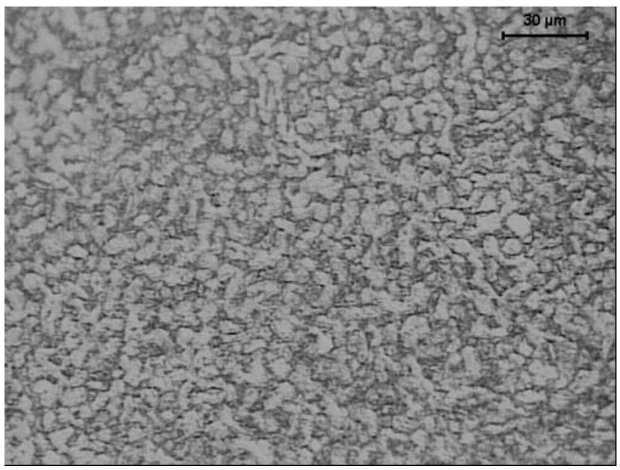

Fig. 1 - Micrograph of Ti-6Al-4V alloy as-received.

The Fig. 2 represents the longitudinal section of the sample tested under creep test at 500ºC, in air with metallic covered. Kroll reagent was used to attack the sample.

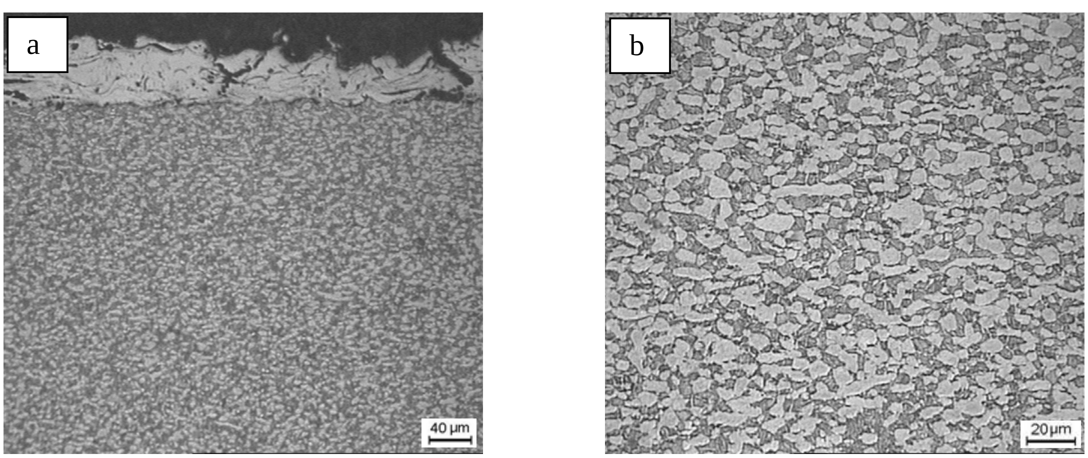

Fig. 2 – Longitudinal section of the sample tested under creep test at 500ºC, in air with metallic coating.

The micrographs show the grain growth of the alpha phase and beta dissolution; based on the initial microstructure before test it was continuous along grain boundaries. It can be considered a mechanism of microstrutural degradation together with the grain growth, formation of oxidation layers and superficial cracks, besides rupture in the coating layer.

The Fig. 3 shows the micrographs obtained by MEV of the coating applied on the Ti-6Al-4V substrate. The thickness of the coating was 0.122 mm to the metallic coating and 0.806 mm to the ceramic coating. Using the semi-quantitative analysis by EDS it can get the composition values from each coating analyzed (Table 1).

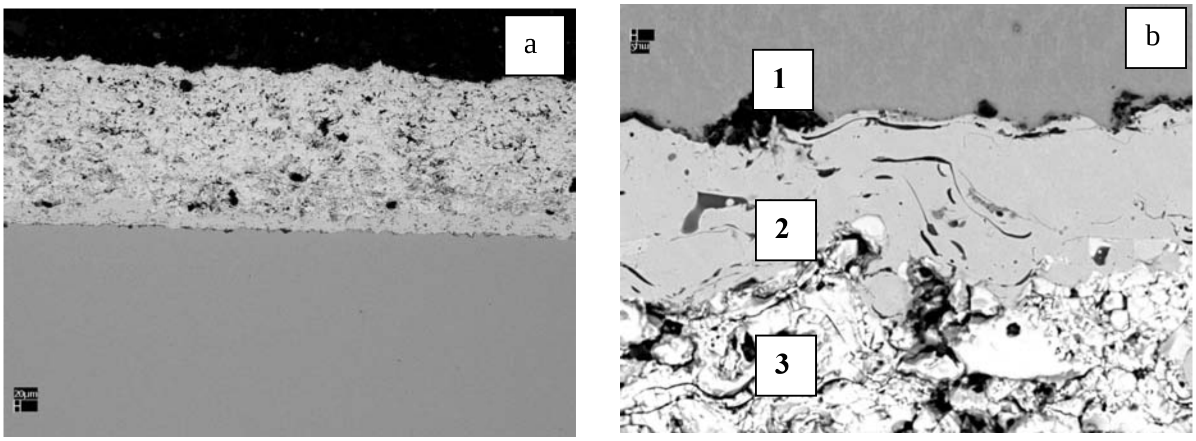

Fig. 3 – Micrographs obtained by MEV of the coating used in the Ti-6Al-4V substrate. a) Deposited coatings on titanium substrate, b) Amplified vision of deposited coatings on titanium substrate: 1) ceramic coating, 2) metallic coating and 3) Ti-6Al-4V substrate.

Table 1 – Semi-quantitative analysis of EDS of the analyzed surfaces.

Elements	Analyzed Surfaces		
	Ceramic Coating (wt %)	Metallic Coating (wt %)	Substrate (wt %)
O	16.06	1.40	2.08
Al	0.17	6.61	5.04
Ti	6.89	6.30	83.67
V	0.32	0.24	4.74
Cr	0.71	19.34	0.49
Co	1.37	32.86	1.08
Ni	1.27	29.07	0.91
Y	5.34	0.65	0.06
Zr	67.87	3.55	1.94

The complementation of the experimental part comprehends a study of the main characteristics of the fracture surfaces. Representative samples from creep tests at 500°C were used to the fractographic analysis.

The Fig. 4 and 5 presents uncoated samples tested under creep test at 500°C in nitrogen atmosphere.

.

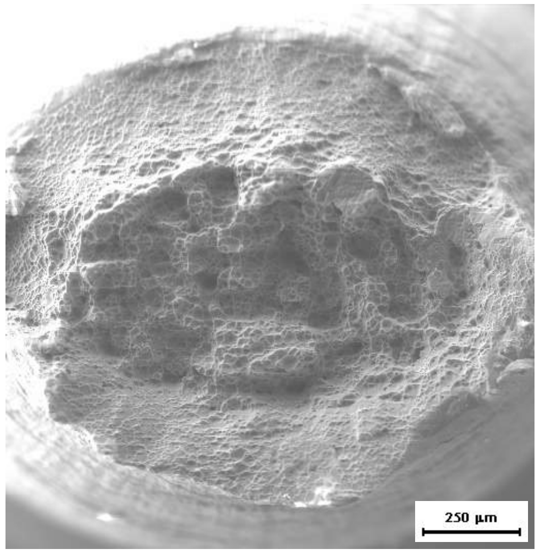

Fig. 4 – General aspect of the fracture surface at 500°C, 520 MPa, uncoated in nitrogen atmosphere.

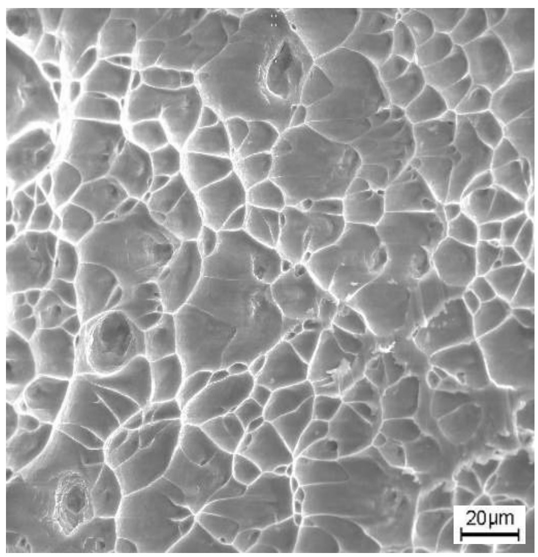

Fig. 5 – Central region of the fracture surface at 500°C, 520 MPa, uncoated in nitrogen atmosphere.

It can be evidenced the narrowing phenomenon and the development of the microcavities. The central region of the fracture surface at 500°C presents a uniform structure with equiaxial shaped dimples and low deep.

The Fig. 6 and 7 presents ceramic coated samples tested under creep test at 500°C in air.

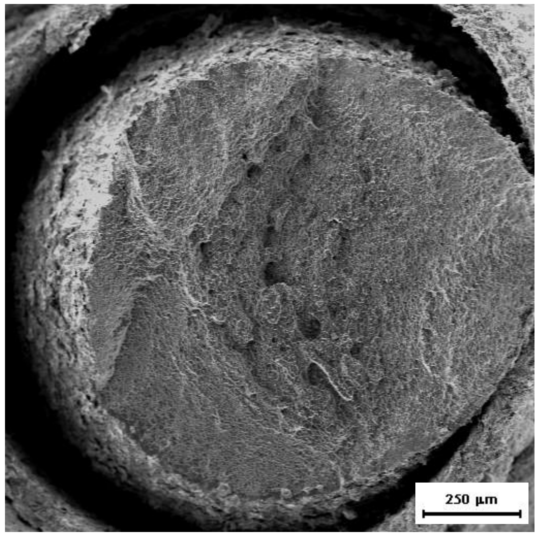

Fig. 6 – General aspect of the fracture surface at 500°C, 520 MPa, with ceramic coating in air.

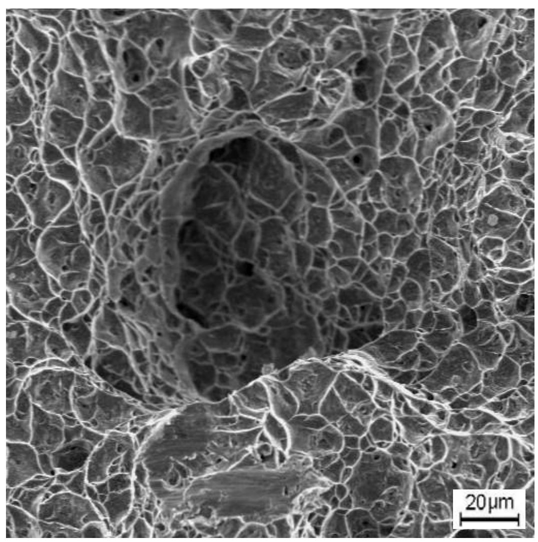

Fig. 7 – Central region of the fracture surface at 500°C, 520 MPa, with ceramic coating in air.

It also observed to the samples with ceramic coating tested in air the narrowing phenomenon and the development of the microcavities. In creep conditions under prolonged temperature effect, the surfaces show accident topography. The ceramic coating near shearing zone doesn’t have a good adherence, characteristics of the transgranular fracture. The fracture surface at 500°C presents a uniform structure with equiaxial shaped dimples and low deep.

The Fig. 8 and 9 presents metallic coated samples tested under creep test at 500°C in air.

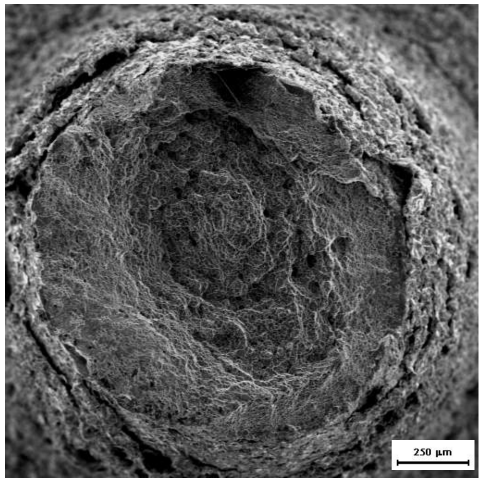

Fig. 8 – General aspect of the fracture surface at 500°C, 520 MPa, with metallic coating in air.

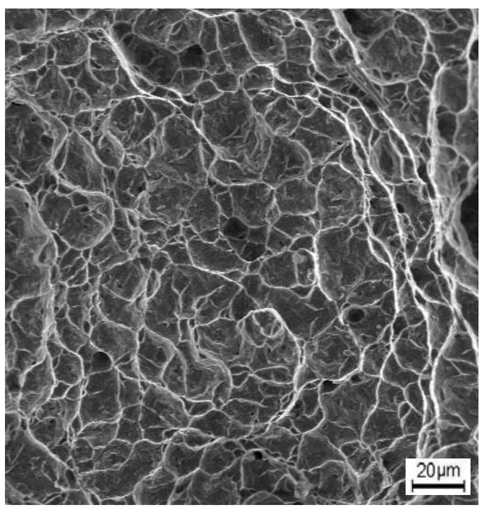

Fig. 9 – Central region of the fracture surface at 500°C, 520 MPa, with metallic coating in air.

The samples with metallic coating tested in air also present the narrowing phenomenon and the development of the microcavities. The fracture surface at 500°C presents a uniform structure and low deep.

The microstructural analyze shows that the predominant mechanism in the test conditions was characterized by formation and coalescence of micro cavities with shape and size varieties. The cavities are corrugated in discontinue regions, like inclusions and points involving dislocation. The size and shape of dimples are governed by number and distribution of nucleated micro cavities and by stress internal level present in the material.

The Fig. 10 presents a sample with ceramic coating tested in creep test at 500°C in air, observed in a stereoscopy to analyze the oxidation effect and the coating degradation.

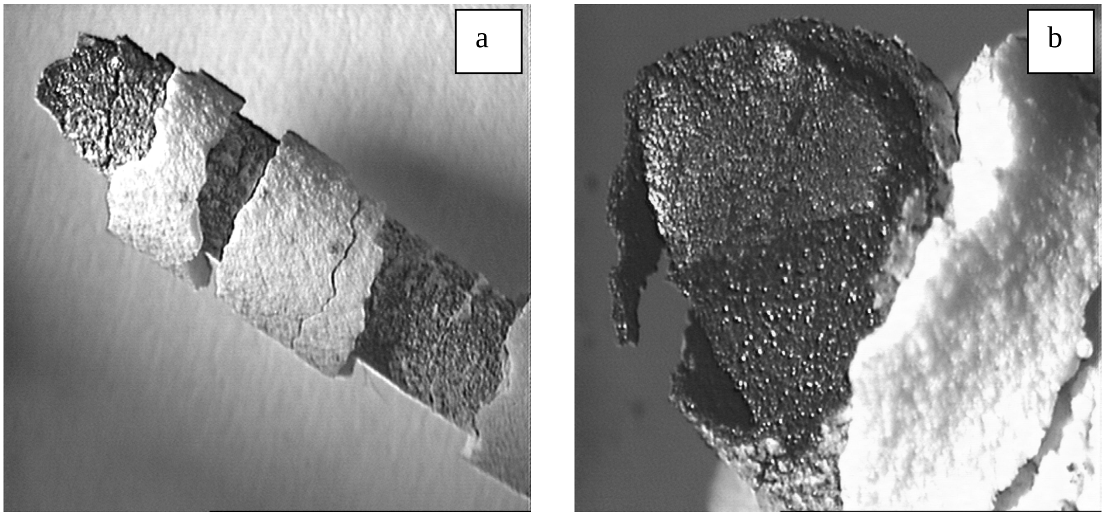

Fig. 10 –Sample tested under creep test at 500°C, 520 MPa, with ceramic coating in air.
Magnitude: 6x (a) and 20x (b).

It can be observed the intense degradation suffered by ceramic and metallic coatings like an effect of the temperature and stress applied. The material suffered a ductile fracture with an irregular rupture.

4. Conclusions

The samples in all conditions analyzed present the narrowing phenomenon and the development of the microcavities. The fracture surface at 500°C presents a uniform structure and low deep. In creep conditions under prolonged temperature effect, the surfaces show accident topography. The ceramic coating near shearing zone doesn't have a good adherence, characteristics of the transgranular fracture.

The microstructural analysis shows that the predominant mechanism in the test conditions was characterized by formation and coalescence of micro cavities with shape and size varieties. The cavities are corrugated in discontinue regions, like inclusions and points involving dislocation. The size and shape of dimples are governed by number and distribution of nucleated microcavities and by stress internal level present in the material. It can be observed the intense degradation suffered by ceramic and metallic coatings like an effect of the temperature and stress applied. The material suffered a ductile fracture with an irregular rupture.

Acknologments

FAPESP (Proc.02/04736-7) for financial support and Rolls-Royce Brasil (São Bernardo do Campo) by plasma-spray coatings.

References

[1] McKee, D.W. and Luthra, K.L. M., 1993, Surface and Coatings Technology, Vol.56, pp. 109-117.
[2] Boyer, R. R., 1996, Mater. Sci. Eng. A, Vol.213, pp. 103.
[3] Abkowitz, S.;Burke, J. J. and Hiltz Jr., R. H., 1955, "Technology of Structural Titanium." D. Van Nostrand Company, pp. 31-32.
[4] Seco, F. J. and Irisarri, A. M., 2001, Fatigue Fract. Eng. Mater. Struc., Vol.24, pp. 741-750.
[5] Gurrappa, I. and Gogia, A. K., 2001, Surface and Coatings Technology, Vol.139, pp. 216-221.
[6] LaPierre, K.; Herman, H. and Tobin, A. G., 1991, Ceram. Eng. Sci. Proc., Vol.12, No. 7-8, pp. 1201-1221.
[7] Xu, H.; Gong, S. and Deng, L., 1998, Thin Solid Films, Vol. 334, pp. 98-102.
[8] Sohn, Y. H.; Lee, E. Y.; Nagaraj, B. A.; Biederman, R. R. and Sisson Jr., R. D., 2001, Surface and Coatings Technology, Vol.146-147, pp. 132-139.
[9] Kucuk, A.; Berndt, C. C.; Senturk, U. and Lima, R. S., 2000, Mater. Sci. Eng. A, Vol.284, pp. 41-50.
[13] Dyson, B. F. and Mc Lean, M., 1990, ISIJ Int., Vol.30, pp. 802-811.
[14] Barboza, M.J.R.; Moura Neto, C.; Silva, C.R.M., 2004, Mater. Sci. Eng. A, Vol.369, pp. 201-209.
[15] Reis, D.A.P.; Silva, C.R.M.; Nono, M.C.A.; Barboza, M.J.R.B.; Piorino, F.; Perez, E.A.C., 2005, Mater. Sci. Eng. A, Vol.399, pp.276-280.